Mayer, Florian; Sampson, William W.; Wloch, Daniela; Mautner, Andreas; Bismarck, Alexander

# Towards the efficient preparation of tough cellulose nanopapers

*Published in:*
Carbohydrate Polymers

*DOI:*
10.1016/j.carbpol.2025.124443

E-pub ahead of print: 15/12/2025

*Document Version*
Publisher's PDF, also known as Version of record

Carbohydrate Polymers 370 (2025) 124443

Contents lists available at ScienceDirect

Carbohydrate Polymers

journal homepage: www.elsevier.com/locate/carbpol

# Towards the efficient preparation of tough cellulose nanopapers

Florian Mayer [a,b], William W. Sampson [c], Daniela Wloch [d], Andreas Mautner [a,e,*], Alexander Bismarck [a,f,g,*]

[a] Institute of Materials Chemistry and Research, Faculty of Chemistry, University of Vienna, Währinger Straße 42, 1090, Vienna, Austria
[b] Department of Bioproducts and Biosystems, Aalto University, Vuorimiehentie 1, 02150, Espoo, Finland
[c] Department of Materials, University of Manchester, Manchester, M13 9PL, UK
[d] Department of Aeronautics, Imperial College London, South Kensington Campus, London, SW7 2AZ, United Kingdom
[e] Institute of Environmental Biotechnology, IFA-Tulln, University of Natural Resources and Life Sciences, Vienna, Konrad-Lorenz-Straße 20, 3430, Tulln an der Donau, Austria
[f] Division of Materials Science, Department of Engineering Sciences and Mathematics, Luleå University of Technology, Luleå, 971 87, Sweden
[g] Department of Chemical Engineering, Imperial College London, South Kensington Campus, London, SW7 2AZ, United Kingdom

ARTICLE INFO

*Keywords:*
Nanocellulose
Nanopaper preparation
Toughness

ABSTRACT

Cellulose nanopapers are attractive materials with outstanding mechanical and optical properties, yet their production is slow. The use of non-aqueous suspension media, in particular ethanol, for nanopaper production reduced filtration times by 73 %. Nanopapers prepared from ethanolic suspensions possessed higher porosities than those prepared from aqueous suspensions, reducing their transparency and tensile properties. Rewetting nanopapers prepared from ethanolic suspensions with water and subsequent drying yielded nanopapers with densities essentially the same as those prepared from aqueous suspensions, which in turn greatly increased mechanical properties and transparency. The strain to failure of rewetted and dried nanopapers prepared from ethanolic suspensions increased from 2.8 % to 7.5 %. The strain to failure of rewetted and dried nanopapers prepared from ethanolic suspensions was also greater than that of nanopapers prepared from aqueous suspensions (3.3 %) albeit at the expense of a 20 % decrease in tensile strength and modulus, which was shown to be attributable to a lower bonding contribution between fibrils in the network. The increased strain to failure results in significantly increased work of fracture. The rewetting and drying treatment also yielded nanopapers with high total luminous transmittance and haze.

## 1. Introduction

Cellulose, and in particular nanocellulose, is among the most prominent research topics in the quest for sustainable, renewable, and green engineering materials with attractive mechanical and barrier properties. Cellulose is naturally produced by green plants, bacteria and even some animals (Moon et al., 2011). Cellulose fibres are a structural component of plants and can be either mechanically or chemically defibrillated to yield cellulose nanofibrils (CNF) (Herrick et al., 1983; Klemm et al., 2005; Saito et al., 2007; Turbak et al., 1982). The widths of CNF usually range from 5 to 60 nm whereas their length can be up to 6 μm (Klemm et al., 2018), thus constituting a nanomaterial with a high aspect ratio and exceptional physical and mechanical properties (Moon et al., 2011; Saito et al., 2013). Films and membranes prepared from CNF are often termed cellulose nanopapers (CNP) and have been widely investigated showing favourable physical and chemical properties such as good chemical stability, low thermal expansion, tuneable optical properties, and high tensile strength and modulus (Henriksson et al., 2008; Miao et al., 2020; Syverud & Stenius, 2008). The possibility to utilise the abundant surface hydroxyl groups of CNF for a variety of chemical modifications such as click-type reactions or the introduction of charged moieties, (Liu et al., 2015; Saito et al., 2007; Thomas et al., 2018) and hence tune the properties of the resulting CNPs, has made them promising candidates for a variety of applications, e.g. separators in, e.g., supercapacitors and fuel cells (Mashkour et al., 2021; Tafete et al., 2022; Zhang et al., 2018). Owing to their excellent oxygen barrier performance and tuneable optical properties CNPs have been explored as alternative packaging materials (Ahankari et al., 2021; Kargarzadeh et al., 2018; Wang et al., 2017).

The three main CNP manufacturing routes currently discussed in

* Corresponding authors.
*E-mail addresses:* andreas.mautner@boku.ac.at (A. Mautner), alexander.bismarck@univie.ac.at (A. Bismarck).

https://doi.org/10.1016/j.carbpol.2025.124443
Received 11 July 2025; Received in revised form 9 September 2025; Accepted 19 September 2025
Available online 21 September 2025

literature are casting, coating and filtration (Liu et al., 2022; Österberg et al., 2013): casting nanocellulose suspensions and evaporating the suspension medium as reported for cellulose nanocrystals for film production by Revol et al. (1992) was adapted by Dufresne et al. (Dufresne et al., 1997) for CNF. This was the first method used to produce CNPs and is still widely utilised at laboratory scale to tune the properties and microstructure of the resulting CNPs by controlling the evaporation parameters and addition of solutes (Hubbe et al., 2017). The coating method usually involves the permanent deposition of a CNF suspension on a porous carrier material to create a hybrid material with CNP (Hubbe et al., 2017) with the drawback, that usually no freestanding CNPs are obtained. Filtration followed by hot pressing allows production of CNPs in analogy to traditional papermaking techniques. The main obstacles for the efficient preparation of CNPs however can be found both in the high viscosity of concentrated CNF suspensions and the high water-retention of CNFs, as these facilitate the need to use very dilute suspensions as feedstock for CNP production, which require substantial amounts of time and energy to dewater by both filtration or evaporation alike (Lindström & Aulin, 2014; Nadeem et al., 2022; Österberg et al., 2013; Sehaqui et al., 2010; Sethi et al., 2021; Sinquefield et al., 2020). The dewatering time of CNPs also increases dramatically with increasing paper grammage and density, further affecting productivity (Hervy et al., 2018) when producing denser or thicker CNPs. Indeed, industrial processes for the high-volume manufacture of tracing paper utilise hot process water to reduce its viscosity and hence increase drainage speed. The dewatering of nanocellulose suspensions is an intensely studied topic and a wide variety of methods have been reported ranging from the use of electro-assisted filtration, surface modification or the addition of salts, to supercritical $CO_2$ drying; the reader is referred to several extensive reviews on the topic (Sinquefield et al., 2020; Solhi et al., 2023). One pathway to reduce the dewatering time of CNF suspensions, which is not as widely reported, is to replace water with other liquids as suspension medium that interact less with the cellulose fibrils or have higher vapour pressures, thus requiring less energy to remove. Although Henriksson et al. (2008) and others Huang et al. (2023); Sim, Ryu, & Youn (2015) have used solvent exchange to facilitate efficient drying of wet filter cakes, the approaches still formed filter cakes from aqueous suspensions. Onyianta et al. (2023) used several solvent exchange and conditioning steps with isopropyl alcohol (IPA) to produce redispersible CNF powders and found that filtration times dropped significantly with increasing IPA content. Most studies reporting on the use of non-aqueous suspension media during CNP preparation, do not document the impacts on the filtration speed but found that the use of lower surface tension solvents influences other properties of the resulting nanopapers, such as porosity, transparency, and haze (Ferguson et al., 2016; Hsieh et al., 2017; Huang et al., 2023; Mautner et al., 2020; Mautner & Bismarck, 2021). Ferguson et al. (2016) reported a correlation between the surface tension of the CNF suspension medium and the resulting CNP porosity, with lower surface tension solvents yielding more porous CNPs. Huang et al. (2023) used solvent exchange to ethanol and hexane after filtration of TEMPO oxidised CNF filter cakes and observed that lower surface tension yielded CNPs with significantly increased pore volumes and larger interlayer pore spaces. Hsieh et al. (2017) reported, that using ethanol as suspension medium during manufacture yielded CNPs with high transparency and haze. Importantly, the use of organic solvents as suspension medium for CNP preparation reduces the mechanical properties of the CNPs significantly (Mautner & Bismarck, 2021). A reduction in density inherently reduces the extent of inter-fibril contact and, thus the tensile strength of the resulting papers. In a classic and seminal contribution, Campbell (1959) postulated that the use of suspension media with different surface tensions could also affect the intrinsic properties of produced papers (and by extension, nanopapers): during removal of the liquid content during drying, capillary forces, which are proportional to the surface tension of the suspension medium, act in interfibril spaces and pull the fibres together. These 'Campbell forces' aid compaction of the resulting fibre network resulting in increased density and hence an increased fibre-fibre bonding area, which, alongside the zero span tensile index directly contributes to the tensile index as elaborated in the theory of Page (1969), which may be stated as:

$$\frac{1}{T} = \frac{9}{8\,Z} + \frac{12\,\delta}{b\,P\,L\,\Phi} \tag{1}$$

where $T$ [kN m kg$^{-1}$] is the specific strength or 'tensile index' of a (nano) paper, $Z$ [kN m kg$^{-1}$] the zero span tensile index, $\delta$ [kg m$^{-1}$] the linear density of nanofibrils with perimeter $P$ [m] and mean length $L$ [m]; $\Phi$ represents the relative bonded area and $b$ [N m$^{-2}$] the shear bond strength per unit area.

The tensile strength of (nano)papers is influenced also by hornification between fibrils during water removal at elevated temperatures, first described by Jayme (1944) as "Verhornung" and further elucidated by Minor (1994), who coined the term "hornification". The absence of water during hot pressing when using non-aqueous suspension media directly influences the hydrogen bond structure of the formed cellulose network, resulting in a less "crosslinked" CNF network (Fernandes Diniz et al., 2004).

The development of strong and tough CNPs has been of great interest in the scientific community, with studies outlining various approaces to achieve this goal. The addition ionic liquids to the suspension medium has recently been reported by Chen et al. (2020) who disclosed that adding 30 wt.-% of 1-ethyl-3-methylimidazolium acetate to the suspension medium yielded CNPs with exceptionally high tensile strength (up to 233 MPa) and modulus of toughness (up to 38 MJ m$^{-3}$), as well as Liu et al. (2025) who reported that the addition of up to 2 wt.-% of various imidazolium based ionic liquids to the suspension medium more than doubled the tensile strength and tensile toughness of produced CNPs. Another promising strategy to increase the ductility and toughness of CNPs is to partially transform the stiff and brittle cellulose I crystal allomorph to the more ductile cellulose II allomorph, either by way of partially dissolving the cellulose fibrils (Abbott & Bismarck, 2010; Gindl & Keckes, 2005) or strong alkaline treatment called mercerization (Mayer et al., 2024; Wloch et al., 2023). While these methods yield CNPs with excellent mechanical properties, they also suffer from the aforementioned drawbacks of CNP production in the form of long dewatering and/or drying times, as well as the consumption of expensive and potentially harmful chemicals. Sethi et al. (2019) reported the use of a hybridization approach combining CNF with non-delignified wood nanofibres to increase the hydrophobicity of the resulting CNPs as well as the nascent filtercake, leading to a significantly increased (75 %) filtration speed and increased water resistance of the resulting CNPs albeit at the cost of tensile properties and yellowing/browning depending on the CNF to wood nanofibre ratio.

In this study, we investigate the potential of using ethanol, a non-aqueous suspension medium that can be considered green and easily accessible, for the efficient and fast production of cellulose nanopapers via filtration. After filtration we conducted a systematic investigation of a family of post-forming treatments using rewetting by water and drying to consolidate the resulting nanopapers and investigate the influence on their physical and mechanical properties. The objective of these post-treatments was to exploit Campbell forces to consolidate and hence densify the intrinsically porous nanopapers filtered from non-aqueous solvents, with a view to increasing their strength and transparency. This approach could offer a route to exploit the faster filtration times offered by film formation from non-aqueous solvents, whilst optimising network properties.

## 2. Experimental

### 2.1. Materials

Cellulose nanofibres (CNF) were produced by mechanical

defibrillation (Granomat JP 150, Fuchs, Switzerland) of never dried, chlorine-free bleached softwood pulp (*picea abies and pinus* spp.) with a composition of 81.3 % cellulose, 12.6 % hemicellulose and 0.3 % ash (Josset et al., 2014) provided by Mercer Stendal (Arneburg, Germany) according to a grinding procedure described in a previous publication (Mayer et al., 2024). The resulting nanofibrils had an average molecular weight $M_w$ of 141.4 kDa, and a crystallinity of ~70 % (Mayer et al., 2024). Ethanol (93.8 wt.-%) denatured with 1 vol.-% of petroleum ether was purchased from Brenntag Austria. If not stated otherwise, deionised water was used in all experiments.

### 2.2. Nanopaper preparation

An overview of the processing parameters and all post processing steps of the nanopapers produced in the subsequent sections is provided in Table 1. For clarity, a schematic overview over the order of manufacturing steps is also provided as Fig. SI 1–1 in section SI 1 of the ESI.

Nanopapers with a nominal areal density of 100 g $m^{-2}$ were prepared following a previously reported method (Mayer et al., 2024), which was slightly modified by using ethanol as the suspension medium. In brief, nanocellulose stock (1.2 g dry mass at a dry matter content of 3.37 wt.-%) was combined with 270 g ethanol (93.8 wt.-%) to reach an ethanol concentration of 85 wt.-%. This suspension was then further diluted with 85 wt.-% ethanol to adjust the volume to exactly 1000 mL (to allow for comparison of the filtration times later on) followed by homogenization via blending (BL-4473, Tristar) at 2000 W for 30 s. The ethanol/CNF suspension was subsequently transferred to a Büchner funnel with a 125 mm diameter fritted glass disk, lined with filter paper (VWR 413, VWR, Leuven, Belgium) and filtered at reduced pressure produced by a water jet pump until a solid filter cake with a matte surface had formed and the flow of suspension medium exiting the Büchner funnel had slowed to one drop per 15 s, which – according to previous experience – yielded filter cakes with a cellulose content of 70–90 %. The resultant dense, yet wet, filter cake was removed from the filter paper, sandwiched between two metal plates, each lined with two layers of blotting paper (3MM Chr VWR, Lutterworth, UK), and pressed at room temperature (23°C) using a hydraulic press (type 25–12-2H, Carver Inc., Wabash, USA) at 1.6 MPa for 30 s to increase its solids content. The cold-pressed filter cake was then placed between two metal plates lined with one layer of blotting paper as cushioning and one layer of release paper and hot pressed in the hydraulic press at 1.6 MPa at 120°C for 15 min to dry and consolidate the network. Of the nine nanopapers filtered from ethanolic suspensions, three were used as reference and thus termed 'Et-CNP-ref', while the rest was used for the production of re-compacted CNPs as described further down.

Another set of nanopapers was prepared as described above from suspensions of CNF in 85 wt.-% ethanol, but the ethanol-wet filter cake was submerged for 5 s in 1 L of deionised water prior to cold pressing – to simulate a short dipping bath in a continuous line process, and to prevent disintegration of the unconsolidated filter cake into the water – followed by hot pressing as described above. These water-dipped Et-CNPs were termed 'Et-CNP-d'.

Reference nanopapers filtered from water were prepared following the same procedure but using water as suspension medium (1.23 g of CNF dry mass in 1000 mL $H_2O$), but. These samples are termed, '$H_2O$-CNP'.

**Table 1**
Sample codes, preparation parameters and eventual Post treatment steps of nanopapers prepared in this study.

| Sample | Preparation Parameters | | Notes | Post treatment |
|---|---|---|---|---|
| | Suspension Medium | CNF dry mass [g] | | |
| $H_2O$-CNP | 1000 mL Water | 1.2 | – | – |
| Et-CNP-Ref | 1000 mL 85 wt.-% EtOH | 1.2 | – | – |
| reEt-CNP-35 | 1000 mL 85 wt.-% EtOH | 1.2 | – | Rewetting and drying at 35 °C |
| reEt-CNP-70 | 1000 mL 85 wt.-% EtOH | 1.2 | – | Rewetting and drying at 70 °C |
| reEt-CNP-110 | 1000 mL 85 wt.-% EtOH | 1.2 | – | Rewetting and drying at 110 °C |
| Et-CNP-d | 1000 mL 85 wt.-% EtOH | 1.2 | Dipped in $H_2O$ prior pressing | – |

### 2.3. Re-compaction of Et-CNPs

To further consolidate cellulose nanopapers produced from ethanolic suspensions they were first submersed in water for 5 min, to allow the nanopaper to fully hydrate but not yet start to disintegrate and subsequently sandwiched between two sheets of blotting paper for 30 s to remove excess water. The still water-wet CNPs were then sandwiched between steel plates, each lined with a sheet of blotting paper and release paper and put under 5 kg-force to prevent cockling during drying. Drying of the wet CNPs was performed at 35°C, 70°C, and 110°C for 30 h, 20 h, and 2 h, respectively, to ensure the nanopapers had fully dried. Consolidated CNPs were termed 'reEt-CNP-X' indicating that they were rewetted and with X denoting the drying temperature. All consolidation experiments were carried out in duplicate.

### 2.4. Moisture content of nanopapers

The moisture content of prepared nanopapers was determined via dynamic vapour sorption (DVS Resolution, Surface Measurement Systems, Wembley, UK). Approximately 20 mg of nanopaper sample were conditioned in the same room as the subsequent mechanical testing was performed (25°C, 40–45 % RH) for 1 week, before entering the system and being dried in water-free air flow for 15 h until no change in weight was detected. The moisture content was calculated from the mass loss during drying.

### 2.5. Thickness, density, and porosity of nanopapers

Thickness $d$ and apparent density $\rho_e$ of all CNPs were determined from specimens cut for tensile testing. From each paper, eight dumbbell-shaped specimens were punched out (Zwick ZCP 020 Manual Cutting Press, Zwick, Ulm, Germany) in a radial pattern evenly distributed across half of each paper to ensure a homogeneous sample composition without bias and to conserve the second half for other tests. The dumbbell-shape (EN ISO 527-2, Type 1BB) had an overall length of 30 mm with a 20 mm long and 2 mm wide parallel section and an overall area $A$ of 85.8 $mm^2$. The thickness $d$ was measured at five points evenly distributed along the specimens' length using a digital micrometer (705–12,229, RS Components, Corby, UK) with a clamping pressure of 150 kPa as the specimens' width was below that required for testing with a conventional paper thickness meter.

Each specimen's mass $m$ was determined using a microbalance (MSA 225P, Sartorius, Göttingen, Germany) and used to calculate the average paper grammage $\Gamma$ (eq. 2), apparent density $\rho_e$ (eq. 3), and hence to estimate porosity $\phi$ (eq. 4) from $A$ and $d$ of the specimens by approximating the skeletal density $\rho_s$ of cellulose I to be 1500 kg $m^{-3}$ (Sehaqui et al., 2011).

$$\Gamma = \frac{m}{A} \tag{2}$$

$$\rho_e = \frac{\Gamma}{d} \tag{3}$$

$$\phi = \left(1 - \frac{\rho_e}{\rho_s}\right) \times 100\% \quad (4)$$

### 2.6. Surface morphology of (consolidated) CNPs

The surface morphology of the produced CNPs was characterised by scanning electron microscopy (SEM) (Supra55VP, Zeiss, Austria) operated at an acceleration voltage of 5 kV and a working distance of 7.4 mm. All specimens were mounted onto aluminium sample holders with carbon tape and coated with an 8 nm layer of 80 % Au and 20 % Pt (Leica SCD 2020/EM QSG 100).

### 2.7. Determining the optical properties of nanopapers

Total luminous transmittance and haze of CNPs were determined using a UV–Vis spectrophotometer (Lambda 356, PerkinElmer LAS Ltd., UK) fitted with a 50 mm integrating sphere in the range of 400 to 700 nm at a scan speed of 240 nm $min^{-1}$ and a slit width of 5 nm.

### 2.8. Determination of tensile properties of nanopapers

Tensile tests were performed on a minimum of ten specimens for each nanopaper sample at 25°C and 40–45 % RH using a dual column universal test frame (Instron Model 5969, Darmstadt, Germany) equipped with a 1 kN load cell, specifically calibrated for low loads. The tensile strain $\varepsilon$ was recorded using an optical non-contact video extensometer (Gig ProE, iMETRUM, Bristol, UK). The gauge length of the test specimen was set at 15 mm, and a crosshead displacement velocity of 1 mm $min^{-1}$ was used. The tensile strength σ was calculated from the measured load, the width and thickness of the specimen. The paper tensile index (cf. specific strength) $T$ was calculated from the load per unit width and the grammage Γ of the specimen and the (grammage corrected) specific modulus M was determined from the linear elastic region of the T vs. $\varepsilon$ curves as a secant between strength values separated by a strain of 0.2 %. The modulus of toughness $K_f$, a measure for the tensile toughness of a material – i.e. the energy a material absorbs during elastic and plastic deformation – (Oh, 2022) was determined by integration of the area under the stress-strain curve of the using the dimensionless strain (eq. 5):

$$K_f = \int_0^{\varepsilon_f} \sigma \mathrm{d}\varepsilon, \quad (5)$$

For comparison we would like to point out, that $K_f$ is in the literature often referred to as work of fracture (Chen et al., 2020; Henriksson et al., 2008; Mayer et al., 2024; Sehaqui et al., 2011; Svagan et al., 2007). However, per definition, the work of fracture is energy per unit area (J $m^{-2}$) while $K_f$ is energy per unit volume (Pa or J $m^{-3}$), which is the quantity termed work of fracture reported in those papers. The modulus of toughness is the work of fracture normalised over the gauge length.

## 3. Results and discussion

### 3.1. Influence of the ethanol content in the suspension medium on the CNP porosity

The results of a preliminary study on the impact of ethanol content in the suspension medium can be found in section SI 2. of the ESI. The results (Fig. SI 2–1), while qualitative in nature, revealed the importance of the surface tension of the suspension medium, affecting the strength of the capillary/Campbell forces acting on the fibril network during drying pulling neighbouring fibrils closer together, improving interfibrillar contact. Above a certain ethanol content in the suspension medium (60 wt.-% to 80 wt.-%) network densification does no longer occur, yielding CNPs with a significantly increased porosity. The dependency on the surface tension of the liquid in the wet filter cake during drying inspired the rewetting and redrying procedure used for the re-consolidation of CNPs described in this study.

Based on the preliminary results (section SI 2 in the ESI), we selected 85 wt.-% ethanol in water mixtures as suspension medium for CNP production, as it represented an ethanol content sufficiently above the observed threshold for high porosity CNPs (Fig. SI 2–1) while facilitating the reuse of the suspension medium by adding only small amounts of 93 wt.-% ethanol to offset the water introduced by the CNF stock.

### 3.2. Filtration times during nanopaper preparation

We compared the filtration times of CNPs prepared from 85 wt.-% ethanol-water suspensions with those of CNPs prepared from pure water suspensions. As baseline, we determined the filtration times of pure water and 85 wt.-% ethanol in water using the same Büchner funnel; within error we observed no difference in the 'filtration' speed for both media (Table SI 3–1 section SI 3 of the ESI). However, once nanocellulose was suspended in either water or 85 wt.-% ethanol, we observed a reduction in average filtration time from 71 ± 3 min to 19 ± 1 min, which can be attributed to a variety of factors simultaneously which all affect the flow of the solvent through the nascent filter cake: the pressure drop acting across the filter cake is the sum of the hydraulic pressure of the suspension medium acting from above and the applied vacuum from below, which was constant over all experiments. However, the hydrostatic pressure ($P = \Delta p + \rho \cdot g \cdot h$) acting from above on the filter cake for water is 20 % greater than for the water-ethanol mixture resulting in a faster compaction of the filter cake in the aqueous suspension resulting in the formation of the initial layers, with high filtration resistance, similar to the findings of Mattsson et al. (2012) at neutral pH and when using a cellulose based filtration membrane. Furthermore, the lower dipole of ethanol compared to water, 1.69 D and 1.86 D, respectively,(Lide, 2003) would result in a significantly reduced interaction between the liquid and the CNFs surface, thus further reducing the filtration resistance and would further reduce the thickness of the hydration shell around the individual cellulose fibrils, thus virtually increasing the porosity of the nascent filter cake. The higher porosity of the ethanolic filter cake leads to a further reduction of the resistance to flow, as described for granular beds by the Kozeny-Carman equation (Carman, 1997). Another factor contributing to the reduced filtration times could be the reduced polarity of the ethanolic suspension medium, reducing the interaction between the fibril surface and the liquid, in analogy to literature utilising different ionic solutions to improve the filtration procedures of (carboxylated) CNFs (Fall et al., 2022; Mautner et al., 2015; Sim, Lee, et al., 2015). These results also suggest that the higher viscosity of ethanol-water mixtures compared to pure water – 1.7 mPa s for 85 wt.-% ethanol/water mixture compared with 1.0 mPa s for pure water (González et al., 2007) – are compensated and even outweighed by the reduced filtration resistance of the forming, more porous filter cake.

### 3.3. Influence of re-consolidation on the physical properties of CNPs

We investigated the impact of paper re-consolidation after forming from ethanolic suspensions as well as dipping of the ethanol wet filter cake in water prior to hot pressing (reEt-CNP-35, 70 & 110 as well as Et-CNP-d, respectively) on the physical properties, such as thickness and density of these CNPs, and compared them to those of reference CNPs produced from aqueous suspensions ($H_2O$-CNP), and from ethanolic suspensions without post treatment (Et-CNP-ref) (Table 2).

The porosity of the untreated Et-CNP-ref sample is almost double that of $H_2O$-CNPs. *t*-Tests revealed that density and porosity of re-consolidated CNPs are not significantly different from those of $H_2O$-CNPs, indicating significant network compaction during secondary drying steps driven by surface tension/Campbell forces leading to a densification of the rewetted fibril network of CNPs formed from ethanolic suspensions. The compaction during the secondary drying appears

**Table 2**
Grammage $\Gamma$, thickness $d$, density $\rho$, and porosity $\phi$ with standard deviation of the different types of CNPs. Note: the grammage was determined by weighing at ambient conditions, thus including sorbed moisture (~4.5–5.9 %).

| Sample | $\Gamma$[g m$^{-2}$] | | | $d$ [μm] | | | $\rho$ [kg m$^{-3}$] | | | $\phi$ [%] | | |
|---|---|---|---|---|---|---|---|---|---|---|---|---|
| Et-CNP-ref | 103.7 | ± | 2.0 | 98.9 | ± | 2.3 | 1049 | ± | 25 | 30.1 | ± | 1.7 |
| reEt-CNP-35 | 113.7 | ± | 2.2 | 91.2 | ± | 2.1 | 1247 | ± | 25 | 16.8 | ± | 1.7 |
| reEt-CNP-70 | 111.9 | ± | 1.4 | 89.1 | ± | 1.8 | 1256 | ± | 32 | 16.3 | ± | 2.1 |
| reEt-CNP-110 | 113.2 | ± | 2.0 | 90.8 | ± | 2.3 | 1247 | ± | 33 | 16.9 | ± | 2.2 |
| Et-CNP-d | 108.2 | ± | 2.0 | 90.4 | ± | 2.6 | 1198 | ± | 32 | 20.1 | ± | 2.1 |
| $H_2O$-CNP | 106.0 | ± | 3.1 | 84.9 | ± | 2.5 | 1248 | ± | 29 | 16.8 | ± | 1.9 |

to be insensitive to the drying temperature and can be attributed to the comparatively higher surface tension of water compared with that of 85 wt.-% ethanol – 72.8 mN m$^{-1}$ vs. ~24 mN m$^{-1}$ for pure water and 85 wt.-% ethanol in water, respectively (Vazquez et al., 1995) – leading to higher Campbell forces during drying; the larger Campbell forces acting on nanofibres in the network exerted by water can overcome the intrinsic fibril network tension, thus pulling neighbouring fibrils closer together and compacting the network. This compaction overwhelmingly occurs in the thickness direction of the papers, as the CNFs are deposited in-plane during filtration. Dipping wet filter cakes produced from ethanolic suspension into water prior to hot pressing resulted in CNPs with higher porosities than those produced from aqueous suspensions indicating that the short dipping time was insufficient to increase the water content of the filter cake sufficiently to produce comparable Campbell forces to those achieved with water alone.

The mechanism of network compaction primarily in the thickness direction of the nanopaper, as reflected by increased density, is apparent in CNP cross-sections (Fig. 1). SE micrographs show a lamellar structure of the prepared CNPs, with Et-CNP-Ref (Fig. 1A) exhibiting numerous significant interlayer pores. These interlayer pores were less pronounced in re-compacted (i.e. reEt-CNP-70, Fig. 1B) CNPs and reference CNPs prepared from aqueous suspensions (i.e. $H_2O$-CNP, Fig. 1C) similar to the findings of Huang et al. (2023) indicating that re-compaction yields nanopapers as dense and compact as if produced directly from aqueous suspensions. SE micrographs of Et-CNP-ref's surface (Fig. 1D) reveal a more porous and open structure than observed in the surfaces of nanopapers produced from aqueous suspensions or re-compacted CNPs formed from ethanolic suspensions ($H_2O$-CNP and reEt-CNP-70 in Fig. 1E & F, respectively). The micrographs also showed a network structure with separated individual fibres being visible in the case of Et-CNP-ref, while all other nanopapers are composed of a tight fibrillar network, consistent with the incidence of inter-layer pores observed in the cross-sections. The differences in the fibril networks clearly illustrate that the presence of water during drying, either in the initial hot-pressing step or during the re-consolidation treatment, resulted in a denser network.

### 3.4. Optical properties of nanopapers before and after re-consolidation

The total luminous transmission of all nanopapers at 572 nm (the wavelength used in the TAPPI T425 standard for the determination of paper opacity) is presented in Fig. 2. Both total luminous transmittance and haze over the full visible light range are shown in section SI 4 of the ESI. All three types of nanopapers, exposed to re-wetting and drying after hot pressing (i.e. Et-CNP-ref, Et-CNP-d and $H_2O$-CNP) exhibited significantly lower total luminous transmittance (Fig. 2) than those nanopapers that were post-treated (reEt-CNP-35/70/110). It is important to note that these nanopapers have lower grammage than those that have been re-wetted and hot-pressed, confirming that their lower transmittance is not caused by more material present in the beam path and can rather be attributable to their greater porosity and hence greater degree of light scattering. Over the full tested spectrum (Fig. SI 4-1 A), reference nanopapers produced by filtration from ethanolic suspensions have the lowest light transmittance (Et-CNP-ref, 10–18 %) followed by nanopapers dipped before hot-pressing (Et-CNP-d, 16–27 %) and those produced from an aqueous CNF suspension (H2O-CNP, 21–32 %).

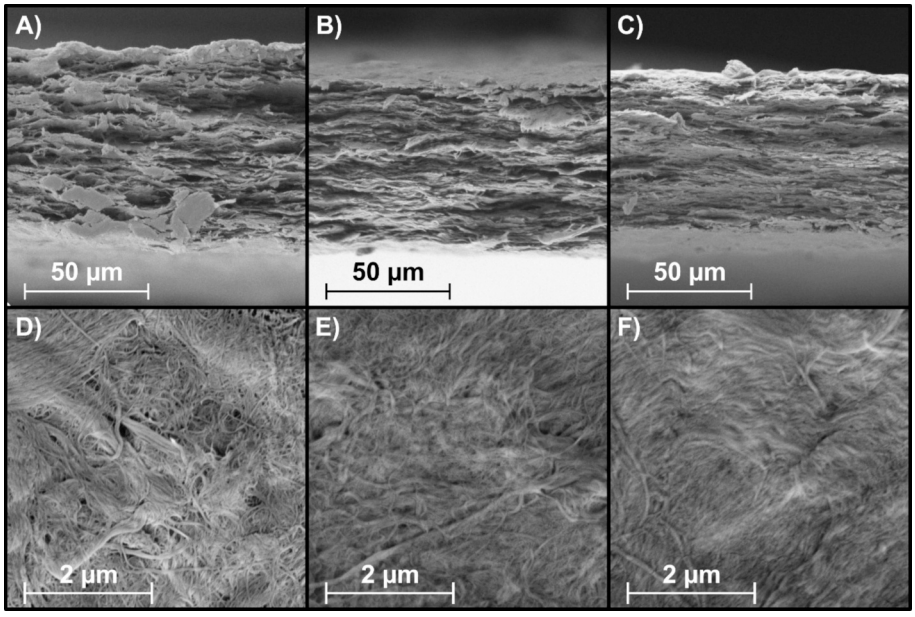


**Fig. 1.** Representative SE micrographs of the nanopaper break edges after tensile testing (top row) and the nanopapers surface of Et-CNP-ref (A & D), reEt-CNP-70 (B & E) and $H_2O$-CNP (C & F).

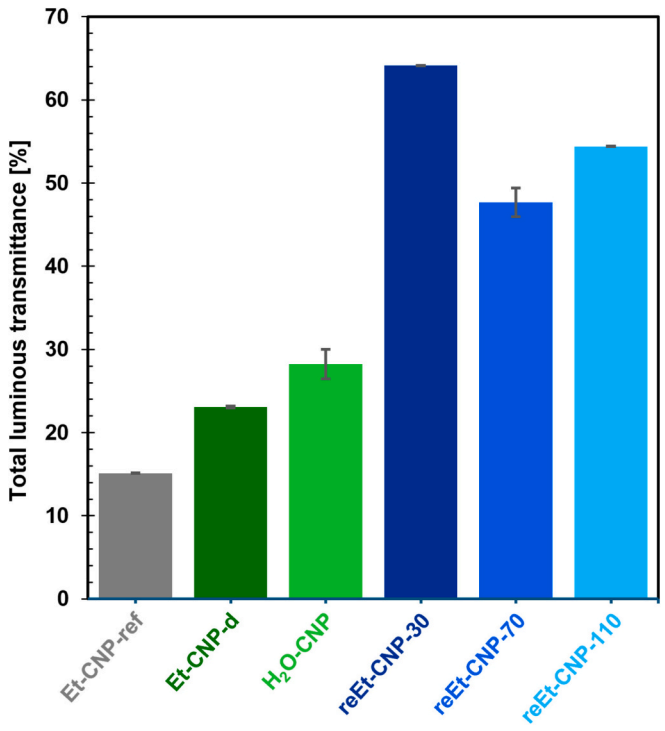


**Fig. 2.** Total luminous transmittance of nanopapers. Error bars represent 95 % confidence intervals.

*Re*-compacted nanopapers possessed a minimum luminous transmittance of 38 % with reEt-CNP-35 (55–69 %) exceeding those of all other nanopapers. To a lesser extent, optical haze (Fig. SI 4-1B) followed the inverse trend of the luminous transmittance and ranged from 84 to 89 % for all nanopapers. Transmittance is determined by light absorption and scattering whereas haze is determined primarily by refraction of incident light. Since the post-treatment process does not change the CNP's composition, we expect absorption differences among our samples to be negligible, so only scattering (i.e. reflection and refraction) is responsible for changes in transmittance and haze. Scattering occurs at interfaces within the network, and the number of interfaces decreased with increasing density. The trends for haze and transmittance found can be attributed to a higher fraction of pores and voids and hence a larger number of interfaces in Et-CNP-ref, which led to more light scattering. The luminous transmittance of all re-wetted and dried nanopapers compared to all other nanopapers (Fig. 2) exceeded that of other nanopapers with similar porosity, consistent with the reduction of scattering sites within the paper caused by network compaction and a "relaxation" of network tensions.

Fig.SI 5–1 in section SI 5 of the ESI shows a qualitative comparison of the coloration all produced CNPs placed on white office paper, showing that the recompaction procedure did not lead to yellowing or other discolorations.

### 3.5. Tensile properties of nanopapers

Fig. 3A shows representative stress-strain curves for all nanopapers and the mechanical properties are summarised in Table 3.

The moisture content of all samples after conditioning for 1 week next to the tensile testing setup was found to be 4.5–5.9 %. All CNPs which were not subjected to re-wetting and drying (i.e. Et-CNP-ref, Et-CNP-d and $H_2O$-CNP) exhibited low strains to failure, $\varepsilon_f$ of 2.5–3.4 % whereas the re-consolidation treatment had a significant impact on the ductility of the resulting nanopapers, more than doubling $\varepsilon_f$ to values up to 7.5 %. The tensile strength of CNPs prepared from aqueous suspensions was significantly higher than that of (re-consolidated) CNPs prepared from ethanolic suspensions. The stress-strain curve of water-dipped Et-CNP-d followed that of CNPs produced from aqueous suspensions ($H_2O$-CNP) yet resulted in premature failure in the plastic deformation region.

In the electronic supplementary information (section SI 6), we provide the manipulation of Eq. 1 to show that the relative difference in the shear bond strength between a pair of nanopapers with different tensile index $T$ and porosity $\phi$ can be estimated:

$$\frac{b_1}{b_2} = \frac{T_1}{T_2}\frac{(Z_c - T_2)}{(Z_c - T_1)}\frac{RBA_1}{RBA_2}, \tag{6}$$

when assuming that $Z_c = 8Z/9$ is unaffected by the use of solvents to form nanopapers. The relative bonded area $RBA$ can be calculated from the porosity $\phi$ of the respective nanopapers as follows (Sampson, 2008):

$$RBA = 1 - \frac{\phi(1-\phi)(2-\phi)}{\ln\left(1/\phi\right)}. \tag{7}$$

The change in shear bond strength per unit area was calculated relative to that of the untreated reference CNPs formed from ethanolic suspensions (i.e. Et-CNP-ref) assuming $Z = 140$ kN m kg$^{-1}$ and is plotted

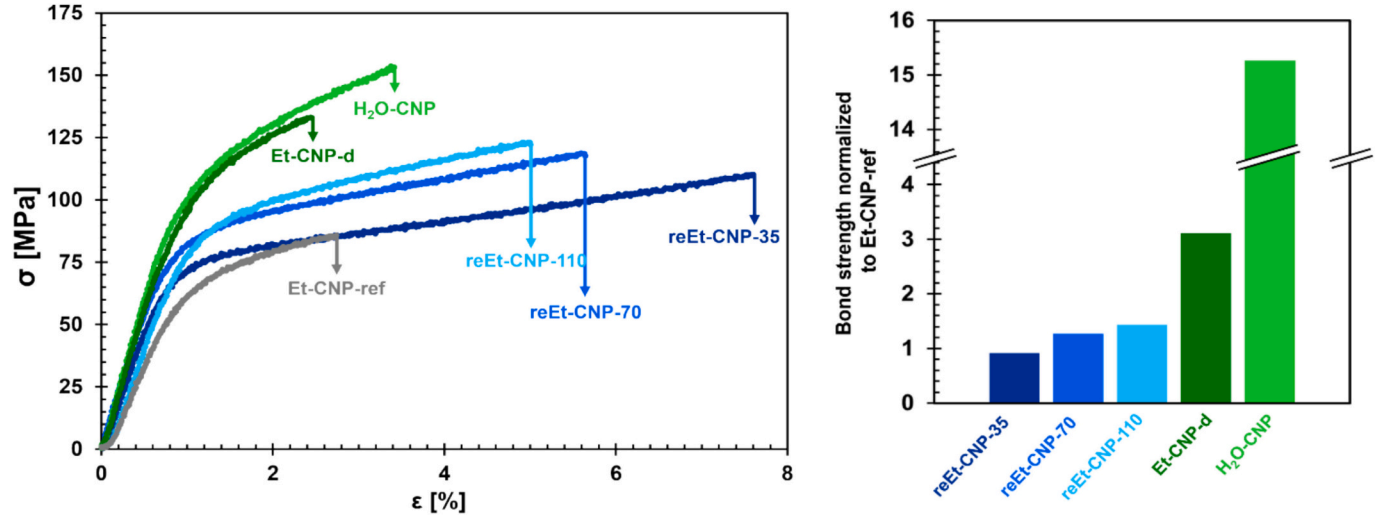


**Fig. 3.** Representative stress-strain curves of all (recompacted) CNPs (A) and the relative bonding contributions to the tensile index normalised to that of Et-CNP-ref (B).

**Table 3**
Tensile index $T$, ultimate tensile strain $\varepsilon_f$, (grammage corrected) specific modulus $M$, and modulus of toughness $K_f$ of nanopapers.

| Sample Name | $T$ [kN m kg$^{-1}$] | | | $\varepsilon_f$ [%] | | | $M$ [MN m kg$^{-1}$] | | | $K_f$ [MJ m$^{-3}$] | | |
|---|---|---|---|---|---|---|---|---|---|---|---|---|
| Et-CNP-ref | 82.5 | ± | 3.4 | 2.8 | ± | 0.4 | 8.4 | ± | 0.6 | 1.7 | ± | 0.4 |
| reEt-CNP-35 | 85.5 | ± | 3.0 | 7.5 | ± | 0.4 | 8.0 | ± | 0.4 | 6.4 | ± | 0.6 |
| reEt-CNP-70 | 93.8 | ± | 3.4 | 5.6 | ± | 0.4 | 9.0 | ± | 0.4 | 5.2 | ± | 0.6 |
| reEt-CNP-110 | 96.4 | ± | 4.0 | 5.1 | ± | 0.6 | 8.4 | ± | 0.6 | 4.7 | ± | 0.6 |
| Et-CNP-d | 104.1 | ± | 4.7 | 2.5 | ± | 0.3 | 9.8 | ± | 0.7 | 2.2 | ± | 0.3 |
| $H_2O$-CNP | 121.1 | ± | 7.1 | 3.3 | ± | 0.5 | 10.4 | ± | 0.6 | 3.6 | ± | 0.8 |

in Fig. 3B. We note that the reported values and trends are very insensitive to the assumed value of $Z$ in the expected range $120 < Z < 150$ kN m kg$^{-1}$. On this basis, we can attribute the increased tensile index of nanopapers re-consolidated at higher drying temperatures (i.e. reEt-CNP-70 and reEt-CNP-110) to an increase in the shear bond strength per unit area.

The significantly higher strain to failure accompanied by relatively small decreases in strength and modulus (Fig. 3A) of CNPs after water rewetting and drying was attributed to network densification (Table 2), which was only associated by marginal increase in interfibrillar bond strength (Fig. 3B) normalised to Et-CNP-ref allowing fibrils to slide over each other until final failure resulting in an increased modulus of toughness. Initial hot pressing of CNF films from ethanolic suspension resulted in poorly consolidated, highly porous nanopapers with fewer connection points between fibrils due to the much-reduced Campbell forces acting on the fibrils during removal of the ethanolic suspension medium. This is consistent with the findings of Hashemzehi et al. (2024) who analysed the degree of hornification of macroscopic cellulose fibres dried from different solvents. Comparing the mechanical properties of CNPs formed from ethanolic suspensions which were rewetted and dried at different temperatures revealed that higher drying temperatures resulted in slightly stronger yet less ductile nanopapers (Table 3). The influence of the drying temperature on the tensile properties was analogous to the temperature dependency of cellulose hornification (Sellman et al., 2023); higher drying temperatures resulted in more hornified samples and thus in a higher bonding contribution (Fig. 3B). The higher strain to failure of rewetted and dried CNPs produced from ethanolic suspensions also resulted in a significantly increased (up to 178 % compared to Et-CNP-ref) modulus of toughness $K_f$ – the area under the stress-strain curve – and thus increased tensile toughness albeit at a slight (~22 %) loss of tensile strength and modulus.

A comparison of the mechanical and optical properties of our CNPs with CNPs manufactured by others can only be made with caution, as both the source of the cellulosic material, as well as other pre-treatment and refinement steps can significantly influence the properties of the resulting nanopapers. With this disclaimer, Fig. 4 juxtaposes the tensile strength σ, and the Young's modulus $E$, of a wide variety of lignocellulosic based CNPs from literature (Du et al., 2020; Fein et al., 2021; Jaiswal et al., 2021; Kontturi et al., 2021; Liu et al., 2023; Mokhena et al., 2021; Rol et al., 2017) and our CNPs.

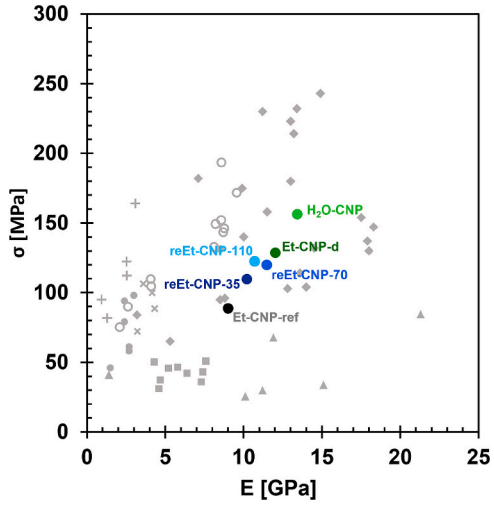


**Fig. 4.** Comparison of the mechanical properties of the CNPs prepared in this study (black, green and blue datapoints) with those of CNPs prepared from lignocellulosic materials using a variety of treatments and preparation methods (grey) reported by Fein et al. (2021) (•), Du et al. (2020) (×), Rol et al. (2017) (▲), Mokhena et al. (2021) (◆), Jaiswal et al. (2021) (■), Liu et al. (2023) (+) and Kontturi et al. (2021) (∘).

## 4. Conclusions

Production of cellulose nanopapers from aqueous suspensions is a time-consuming process. Using ethanol-water mixtures as a suspension medium for CNF allowed for a drastic reduction of filtration times due to the formation of a more porous filter cake reducing the overall filtration resistance. Nanopapers produced from ethanolic filter cakes had much higher porosities and thus significantly lower mechanical properties than papers produced from water-wet filter cakes, because of much lower Campbell forces acting on the drying fibril network. We showed that rewetting with water and drying of CNPs produced from ethanolic suspensions led to significant network compaction, increasing the paper density but only slightly the bonding contribution, resulted in CNPs with increased tensile strength and strain to failure. While having an overall lower tensile strength and modulus compared to papers produced from aqueous suspensions, CNPs produced from ethanol-water mixtures exhibited a significant increase in their strain to failure and modulus of toughness, and thus, tensile toughness. The compaction of the fibril network during rewetting and drying yielded high haze nanopapers with a much higher optical transmittance than CNPs produced from aqueous suspensions.

## CRediT authorship contribution statement

**Florian Mayer:** Writing – review & editing, Writing – original draft, Visualization, Validation, Methodology, Investigation, Formal analysis, Data curation, Conceptualization. **William W. Sampson:** Writing – review & editing, Validation, Methodology, Formal analysis. **Daniela Wloch:** Writing – review & editing, Methodology, Investigation, Data curation. **Andreas Mautner:** Writing – review & editing, Writing – original draft, Validation, Supervision, Project administration. **Alexander Bismarck:** Writing – review & editing, Writing – original draft, Validation, Supervision, Resources, Methodology, Funding acquisition, Conceptualization.

## Declaration of competing interest

The authors declare the following financial interests/personal relationships which may be considered as potential competing interests: Alexander Bismarck reports financial support was provided by University of Vienna. Florian Mayer reports financial support was provided by University of Vienna. Alexander Bismarck reports a relationship with University of Vienna that includes: employment. Florian Mayer reports a

relationship with University of Vienna that includes: employment. William Sampson reports a relationship with The University of Manchester that includes: employment. Andreas Mautner reports a relationship with University of Natural Resources and Life Sciences Vienna that includes: employment. Daniela Wloch reports a relationship with Imperial College London that includes: employment. NA If there are other authors, they declare that they have no known competing financial interests or personal relationships that could have appeared to influence the work reported in this paper.

## Acknowledgements

We are grateful to Mag. Dr. Stefan Puchegger of the Faculty Center for Nanostructure Research at the University of Vienna for his help and guidance in using the SEM, Klaus Ritter for the preliminary experiments, which motivated us to further investigate the effect of rewetting of nanopapers, and Fabian Edinger for assistance in determining the CNF-free filtration speed. F.M. is grateful to the University of Vienna and the Institute of Materials Chemistry for funding (#371300).

## Appendix A. Supplementary data

Supplementary data to this article can be found online at https://doi.org/10.1016/j.carbpol.2025.124443.

## Data availability

Data will be made available on request.

## References

Abbott, A., & Bismarck, A. (2010). Self-reinforced cellulose nanocomposites. *Cellulose, 17*(4), 779–791. https://doi.org/10.1007/s10570-010-9427-5

Ahankari, S. S., Subhedar, A. R., Bhadauria, S. S., & Dufresne, A. (2021). Nanocellulose in food packaging: A review. *Carbohydrate Polymers, 255*, Article 117479. https://doi.org/10.1016/j.carbpol.2020.117479

Campbell, W. B. (1959). The mechanism of bonding. *Tappi, 42*(12). https://doi.org/10.32964/tj42.12.999

Carman, P. C. (1997). Fluid flow through granular beds. *Chemical Engineering Research and Design, 75*, S32–S48. https://doi.org/10.1016/s0263-8762(97)80003-2

Chen, F., Xiang, W., Sawada, D., Bai, L., Hummel, M., Sixta, H., & Budtova, T. (2020). Exploring Large Ductility in Cellulose Nanopaper Combining High Toughness and Strength. *ACS Nano, 14*(9), 11150–11159. https://doi.org/10.1021/acsnano.0c02302

Du, H., Parit, M., Wu, M., Che, X., Wang, Y., Zhang, M., … Li, B. (2020). Sustainable valorization of paper mill sludge into cellulose nanofibrils and cellulose nanopaper. *Journal of Hazardous Materials, 400*, Article 123106. https://doi.org/10.1016/j.jhazmat.2020.123106

Dufresne, A., Cavaillé, J.-Y., & Vignon, M. R. (1997). Mechanical behavior of sheets prepared from sugar beet cellulose microfibrils. *Journal of Applied Polymer Science, 64*(6), 1185–1194. https://doi.org/10.1002/(sici)1097-4628(19970509)64:6<1185::Aid-app19>3.0.Co;2-v

Fall, A., Henriksson, M., Karppinen, A., Opstad, A., Heggset, E. B., & Syverud, K. (2022). The effect of ionic strength and pH on the dewatering rate of cellulose nanofibril dispersions. *Cellulose, 29*(14), 7649–7662. https://doi.org/10.1007/s10570-022-04719-y

Fein, K., Bousfield, D. W., & Gramlich, W. M. (2021). Processing Effects on Structure, Strength, and Barrier Properties of Refiner-Produced Cellulose Nanofibril Layers. *ACS Applied Polymer Materials, 3*(7), 3666–3678. https://doi.org/10.1021/acsapm.1c00620

Ferguson, A., Khan, U., Walsh, M., Lee, K. Y., Bismarck, A., Shaffer, M. S., … Bergin, S. D. (2016). Understanding the dispersion and assembly of bacterial cellulose in organic solvents. *Biomacromolecules, 17*(5), 1845–1853. https://doi.org/10.1021/acs.biomac.6b00278

Fernandes Diniz, J. M. B., Gil, M. H., & Castro, J. A. A. M. (2004). Hornification - its origin and interpretation in wood pulps. *Wood Science and Technology, 37*(6), 489–494. https://doi.org/10.1007/s00226-003-0216-2

Gindl, W., & Keckes, J. (2005). All-cellulose nanocomposite. *Polymer, 46*(23), 10221–10225. https://doi.org/10.1016/j.polymer.2005.08.040

González, B., Calvar, N., Gómez, E., & Domínguez, Á. (2007). Density, dynamic viscosity, and derived properties of binary mixtures of methanol or ethanol with water, ethyl acetate, and methyl acetate at T=(293.15, 298.15, and 303.15)K. *Journal of Chemical Thermodynamics, 39*(12), 1578–1588. https://doi.org/10.1016/j.jct.2007.05.004

Hashemzehi, M., Sjöstrand, B., Håkansson, H., & Henriksson, G. (2024). Degrees of hornification in softwood and hardwood kraft pulp during drying from different solvents. *Cellulose, 31*(3), 1813–1825. https://doi.org/10.1007/s10570-023-05657-z

Henriksson, M., Berglund, L. A., Isaksson, P., Lindstrom, T., & Nishino, T. (2008). Cellulose nanopaper structures of high toughness. *Biomacromolecules, 9*(6), 1579–1585. https://doi.org/10.1021/bm800038n

Herrick, F. W., Casebier, R. L., Hamilton, J. K., & Sandberg, K. R. (1983). Microfibrillated cellulose: Morphology and accessibility. *Journal of Applied Polymer Science: Applied Polymer Symposium*, 1983-01-01. United States.

Hervy, M., Bock, F., & Lee, K.-Y. (2018). Thinner and better: (Ultra-)low grammage bacterial cellulose nanopaper-reinforced polylactide composite laminates. *Composites Science and Technology, 167*, 126–133. https://doi.org/10.1016/j.compscitech.2018.07.027

Hsieh, M. C., Koga, H., Suganuma, K., & Nogi, M. (2017). Hazy transparent cellulose nanopaper. *Scientific Reports, 7*, Article 41590. https://doi.org/10.1038/srep41590

Huang, Y., Kasuga, T., Nogi, M., & Koga, H. (2023). Clearly transparent and air-permeable nanopaper with porous structures consisting of TEMPO-oxidized cellulose nanofibers. *RSC Advances, 13*(31), 21494–21501. https://doi.org/10.1039/d3ra03840h

Hubbe, M. A., Ferrer, A., Tyagi, P., Yin, Y., Salas, C., Pal, L., & Rojas, O. J. (2017). Nanocellulose in thin films, coatings, and plies for packaging applications: A review. *Bioresources, 12*(1), 2143–2233. https://doi.org/10.15376/biores.12.1.2143-2233

Jaiswal, A. K., Kumar, V., Khakalo, A., Lahtinen, P., Solin, K., Pere, J., & Toivakka, M. (2021). Rheological behavior of high consistency enzymatically fibrillated cellulose suspensions. *Cellulose, 28*(4), 2087–2104. https://doi.org/10.1007/s10570-021-03688-y

Jayme, G. (1944). Mikro-quellungsmessungen an Zellstoffen. *Wochenblatt Der Papierfabrikanten, 6*, 187–194.

Josset, S., Orsolini, P., Siqueira, G., Tejado, A., Tingaut, P., & Zimmermann, T. (2014). Energy consumption of the nanofibrillation of bleached pulp, wheat straw and recycled newspaper through a grinding process. *Nordic Pulp & Paper Research Journal, 29*(1), 167–175. https://doi.org/10.3183/npprj-2014-29-01-p167-175

Kargarzadeh, H., Huang, J., Lin, N., Ahmad, I., Mariano, M., Dufresne, A., Thomas, S., & Gałęski, A. (2018). Recent developments in nanocellulose-based biodegradable polymers, thermoplastic polymers, and porous nanocomposites. *Progress in Polymer Science, 87*, 197–227. https://doi.org/10.1016/j.progpolymsci.2018.07.008

Klemm, D., Heublein, B., Fink, H. P., & Bohn, A. (2005). Cellulose: fascinating biopolymer and sustainable raw material. *Angewandte Chemie, International Edition in English, 44*(22), 3358–3393. https://doi.org/10.1002/anie.200460587

Klemm, D., Cranston, E. D., Fischer, D., Gama, M., Kedzior, S. A., Kralisch, D., … Rauchfuß, F. (2018). Nanocellulose as a natural source for groundbreaking applications in materials science: Today's state. *Materials Today, 21*(7), 720–748. https://doi.org/10.1016/j.mattod.2018.02.001

Kontturi, K. S., Lee, K.-Y., Jones, M. P., Sampson, W. W., Bismarck, A., & Kontturi, E. (2021). Influence of biological origin on the tensile properties of cellulose nanopapers. *Cellulose, 28*(10), 6619–6628. https://doi.org/10.1007/s10570-021-03935-2

Lide, D. R. (2003). In D. R. Lide (Ed.), *CRC Handbook of Chemistry and Physics* (84 ed.). CRC Press https://books.google.at/books?id=kSXzwAEACAAJ.

Lindström, T., & Aulin, C. (2014). Market and technical challenges and opportunities in the area of innovative new materials and composites based on nanocellulosics. *Scandinavian Journal of Forest Research, 29*(4), 345–351. https://doi.org/10.1080/02827581.2014.928365

Liu, P., Borrell, P. F., Bozic, M., Kokol, V., Oksman, K., & Mathew, A. P. (2015). Nanocelluloses and their phosphorylated derivatives for selective adsorption of Ag(+), Cu(2+) and Fe(3+) from industrial effluents. *Journal of Hazardous Materials, 294*, 177–185. https://doi.org/10.1016/j.jhazmat.2015.04.001

Liu, W., Liu, K., Du, H., Zheng, T., Zhang, N., Xu, T., Pang, B., Zhang, X., Si, C., & Zhang, K. (2022). Cellulose Nanopaper: Fabrication, Functionalization, and Applications. *Nano-Micro Letters, 14*(1), 104. https://doi.org/10.1007/s40820-022-00849-x

Liu, W., Zhang, S., Liu, K., Yang, H., Lin, Q., Xu, T., Song, X., Du, H., Bai, L., Yao, S., & Si, C. (2023). Sustainable preparation of lignocellulosic nanofibrils and cellulose nanopaper from poplar sawdust. *Journal of Cleaner Production, 384*. https://doi.org/10.1016/j.jclepro.2022.135582

Liu, Y., Feng, S., Zhang, Z., Meng, Q., & Shi, X. (2025). Strong and tough cellulose nanopapers enabled by imidazolium ionic liquids. *Cellulose, 32*(12), 7067–7081. https://doi.org/10.1007/s10570-025-06678-6

Mashkour, M., Rahimnejad, M., Mashkour, M., & Soavi, F. (2021). Increasing bioelectricity generation in microbial fuel cells by a high-performance cellulose-based membrane electrode assembly. *Applied Energy, 282*. https://doi.org/10.1016/j.apenergy.2020.116150

Mattsson, T., Sedin, M., & Theliander, H. (2012). Filtration properties and skin formation of micro-crystalline cellulose. *Separation and Purification Technology, 96*, 139–146. https://doi.org/10.1016/j.seppur.2012.05.029

Mautner, A., & Bismarck, A. (2021). Bacterial nanocellulose papers with high porosity for optimized permeance and rejection of nm-sized pollutants. *Carbohydrate Polymers, 251*, Article 117130. https://doi.org/10.1016/j.carbpol.2020.117130

Mautner, A., Lee, K.-Y., Tammelin, T., Mathew, A. P., Nedoma, A. J., Li, K., & Bismarck, A. (2015). Cellulose nanopapers as tight aqueous ultra-filtration membranes. *Reactive and Functional Polymers, 86*, 209–214. https://doi.org/10.1016/j.reactfunctpolym.2014.09.014

Mautner, A., Nawawi, W. M. F. W., Lee, K.-Y., & Bismarck, A. (2020). High porosity cellulose nanopapers as reinforcement in multi-layer epoxy laminates. *Composites Part A Applied Science and Manufacturing, 131*. https://doi.org/10.1016/j.compositesa.2020.105779

Mayer, F., Prado-Roller, A., Mautner, A., & Bismarck, A. (2024). Retain strength, gain ductility: tough and transparent nanopapers by mercerisation. *Cellulose, 31*(3), 1533–1544. https://doi.org/10.1007/s10570-023-05714-7

Miao, C., Du, H., Parit, M., Jiang, Z., Tippur, H. V., Zhang, X., … Wang, R. (2020). Superior crack initiation and growth characteristics of cellulose nanopapers. *Cellulose, 27*(6), 3181–3195. https://doi.org/10.1007/s10570-020-03015-x

Minor, J. L. (1994). Hornification-its origin and meaning. *Progress in Paper Recycling, 3*(2), 93–95.

Mokhena, T. C., Sadiku, E. R., Mochane, M. J., Ray, S. S., John, M. J., & Mtibe, A. (2021). Mechanical properties of cellulose nanofibril papers and their bionanocomposites: A review. *Carbohydrate Polymers, 273*, Article 118507. https://doi.org/10.1016/j.carbpol.2021.118507

Moon, R. J., Martini, A., Nairn, J., Simonsen, J., & Youngblood, J. (2011). Cellulose nanomaterials review: Structure, properties and nanocomposites. *Chemical Society Reviews, 40*(7), 3941–3994. https://doi.org/10.1039/c0cs00108b

Nadeem, H., Dehghani, M., Garnier, G., & Batchelor, W. (2022). Life cycle assessment of cellulose nanofibril films via spray deposition and vacuum filtration pathways for small scale production. *Journal of Cleaner Production, 342*. https://doi.org/10.1016/j.jclepro.2022.130890

Oh, G. (2022). A simplified toughness estimation method based on standard tensile data. *International Journal of Pressure Vessels and Piping, 199*. https://doi.org/10.1016/j.ijpvp.2022.104733

Onyianta, A. J., Xu, G., Etale, A., Eloi, J. C., & Eichhorn, S. J. (2023). Tackling the challenge of drying and redispersion of cellulose nanofibrils via membrane-facilitated liquid phase exchange. *Carbohydrate Polymers, 314*, Article 120943. https://doi.org/10.1016/j.carbpol.2023.120943

Österberg, M., Vartiainen, J., Lucenius, J., Hippi, U., Seppala, J., Serimaa, R., & Laine, J. (2013). A fast method to produce strong NFC films as a platform for barrier and functional materials. *ACS Applied Materials & Interfaces, 5*(11), 4640–4647. https://doi.org/10.1021/am401046x

Page, D. (1969). A theory for the tensile strength of paper. *Tappi, 52*, 674–681.

Revol, J. F., Bradford, H., Giasson, J., Marchessault, R. H., & Gray, D. G. (1992). Helicoidal self-ordering of cellulose microfibrils in aqueous suspension. *International Journal of Biological Macromolecules, 14*(3), 170–172. https://doi.org/10.1016/s0141-8130(05)80008-x

Rol, F., Karakashov, B., Nechyporchuk, O., Terrien, M., Meyer, V., Dufresne, A., … Bras, J. (2017). Pilot-Scale Twin Screw Extrusion and Chemical Pretreatment as an Energy-Efficient Method for the Production of Nanofibrillated Cellulose at High Solid Content. *ACS Sustainable Chemistry & Engineering, 5*(8), 6524–6531. https://doi.org/10.1021/acssuschemeng.7b00630

Saito, T., Kimura, S., Nishiyama, Y., & Isogai, A. (2007). Cellulose nanofibers prepared by TEMPO-mediated oxidation of native cellulose. *Biomacromolecules, 8*(8), 2485–2491. https://doi.org/10.1021/bm0703970

Saito, T., Kuramae, R., Wohlert, J., Berglund, L. A., & Isogai, A. (2013). An ultrastrong nanofibrillar biomaterial: the strength of single cellulose nanofibrils revealed via sonication-induced fragmentation. *Biomacromolecules, 14*(1), 248–253. https://doi.org/10.1021/bm301674e

Sampson, W. (2008). Unified theory for structural statistics of flocculated and random fibre networks. *Journal of Pulp and Paper Science, 34*(2), 91.

Sehaqui, H., Liu, A., Zhou, Q., & Berglund, L. A. (2010). Fast preparation procedure for large, flat cellulose and cellulose/inorganic nanopaper structures. *Biomacromolecules, 11*(9), 2195–2198. https://doi.org/10.1021/bm100490s

Sehaqui, H., Zhou, Q., Ikkala, O., & Berglund, L. A. (2011). Strong and tough cellulose nanopaper with high specific surface area and porosity. *Biomacromolecules, 12*(10), 3638–3644. https://doi.org/10.1021/bm2008907

Sellman, F. A., Benselfelt, T., Larsson, P. T., & Wagberg, L. (2023). Hornification of cellulose-rich materials - A kinetically trapped state. *Carbohydrate Polymers, 318*, Article 121132. https://doi.org/10.1016/j.carbpol.2023.121132

Sethi, J., Visanko, M., Osterberg, M., & Sirvio, J. A. (2019). A fast method to prepare mechanically strong and water resistant lignocellulosic nanopapers. *Carbohydrate Polymers, 203*, 148–156. https://doi.org/10.1016/j.carbpol.2018.09.037

Sethi, J., Liimatainen, H., & Sirvio, J. A. (2021). Fast and Filtration-Free Method to Prepare Lactic Acid-Modified Cellulose Nanopaper. *ACS Omega, 6*(29), 19038–19044. https://doi.org/10.1021/acsomega.1c02328

Sim, K., Lee, J., Lee, H., & Youn, H. J. (2015). Flocculation behavior of cellulose nanofibrils under different salt conditions and its impact on network strength and dewatering ability. *Cellulose, 22*(6), 3689–3700. https://doi.org/10.1007/s10570-015-0784-y

Sim, K., Ryu, J., & Youn, H. J. (2015). Structural characteristics of nanofibrillated cellulose mats: Effect of preparation conditions. *Fibers and Polymers, 16*(2), 294–301. https://doi.org/10.1007/s12221-015-0294-4

Sinquefield, S., Ciesielski, P. N., Li, K., Gardner, D. J., & Ozcan, S. (2020). Nanocellulose Dewatering and Drying: Current State and Future Perspectives. *ACS Sustainable Chemistry & Engineering, 8*(26), 9601–9615. https://doi.org/10.1021/acssuschemeng.0c01797

Solhi, L., Guccini, V., Heise, K., Solala, I., Niinivaara, E., Xu, W., … Kontturi, E. (2023). Understanding Nanocellulose-Water Interactions: Turning a Detriment into an Asset. *Chemical Reviews, 123*(5), 1925–2015. https://doi.org/10.1021/acs.chemrev.2c00611

Svagan, A. J., Samir, M. A., & Berglund, L. A. (2007). Biomimetic polysaccharide nanocomposites of high cellulose content and high toughness. *Biomacromolecules, 8*(8), 2556–2563. https://doi.org/10.1021/bm0703160

Syverud, K., & Stenius, P. (2008). Strength and barrier properties of MFC films. *Cellulose, 16*(1), 75–85. https://doi.org/10.1007/s10570-008-9244-2

Tafete, G. A., Abera, M. K., & Thothadri, G. (2022). Review on nanocellulose-based materials for supercapacitors applications. *Journal of Energy Storage, 48*. https://doi.org/10.1016/j.est.2021.103938

Thomas, B., Raj, M. C., B, A. K., H, R. M., Joy, J., Moores, A., … Sanchez, C. (2018). Nanocellulose, a versatile green platform: From biosources to materials and their applications. *Chemical Reviews, 118*(24), 11575–11625. https://doi.org/10.1021/acs.chemrev.7b00627

Turbak, A. F., Snyder, F. W., & Sandberg, K. R. (1982). Microfibrillated cellulose, a new cellulose product: properties, uses, and commercial potential. In *9. cellulose conference*, 1983-01-01. Syracuse, NY, USA.

Vazquez, G., Alvarez, E., & Navaza, J. M. (1995). Surface tension of alcohol water + water from 20 to 50.degree.C. *Journal of Chemical and Engineering Data, 40*(3), 611–614. https://doi.org/10.1021/je00019a016

Wang, J., Gardner, D. J., Stark, N. M., Bousfield, D. W., Tajvidi, M., & Cai, Z. (2017). Moisture and oxygen barrier properties of cellulose nanomaterial-based films. *ACS Sustainable Chemistry & Engineering, 6*(1), 49–70. https://doi.org/10.1021/acssuschemeng.7b03523

Wloch, D., Herrera, N., & Lee, K.-Y. (2023). Optically transparent laminated acrylic composites reinforced with mercerised bacterial cellulose nanopaper. *Composites Part A Applied Science and Manufacturing, 172*. https://doi.org/10.1016/j.compositesa.2023.107583

Zhang, Y., Zhang, L., Cui, K., Ge, S., Cheng, X., Yan, M., Yu, J., & Liu, H. (2018). Flexible Electronics Based on Micro/Nanostructured Paper. *Advanced Materials, 30*(51), Article e1801588. https://doi.org/10.1002/adma.201801588